PLISKA
STUDIA MATHEMATICA

ПЛИСКА
МАТЕМАТИЧЕСКИ СТУДИИ

Pliska Stud. Math. **26** (2016), 155–163

PLISKA
STUDIA MATHEMATICA

AERODYNAMIC CHARACTERISTICS OF JOUKOWSKY LIKE WINGS

Yoshihiro Mochimaru

Aerodynamic characteristics of Joukowsky like airfoils are analyzed, under the assumption that the flow near the airfoil is governed by two-dimensional incompressible isothermal Newtonian fluid flow, beyond the viscous boundary-layer of which is approximated by a potential flow with a new parameter. Vorticity transport equation is solved numerically, using a spectral finite difference scheme to give steady-state various characteristics.

1. Introduction

Aerodynamic characteristics of airfoils were investigated experimentally by M. M. Munk [1], E. N. Jacobs [2], E. M. Jacobs & I. H. Abbott [3], E. A. Jacobs, K. E. Ward, R. M. Pinkerton [4], E. A. Jacobs & A. Sherman [5], R. H. Neely, T. V. Bollech, G. C. Westrick, R. R. Graham [6], H. C. Garner & A. S. Baston [7]. At an early stage, under a frictionless incompressible flow assumption, analytical estimation of wing shape effect was presented by M. M. Munk [8], T. Theodorsen [9]. I. H. Abbott & A. E. Doenhoff published an accumulated book [10]. Also data on aerodynamic characteristics of airfoils were found in Ref. [11].

In this paper analyzed is a flow near the surface of Joukowsky-like airfoil, which is assumed to be two-dimensional and governed by incompressible isothermal Newtonian fluid flow. All the more beyond the viscous boundary-layer the speed of the flow is high so as to be of potential flow, which is uniform far away from the airfoil.

2010 *Mathematics Subject Classification:* 31A35, 33E05, 65N06, 76D05.
Key words: Jpukowsky airfoil, wing, numerical simulation.

2. Analysis

2.1. Configuration and coordinate system

The space around a Joukowsky-like airfoil is assumed to be given by the dimensionless Cartesian coordinate (x, y) (based on the reference length L) through a conformal mapping system (α, β)

$$x + iy \equiv z = q\left(\zeta^* + \frac{c_1}{\zeta^*} + \frac{c_2}{\zeta^{*2}}\right), \ (q, c_1, c_2 : \text{ real constants}),$$

$$\zeta^* = \zeta_0 + (1 - \zeta_0)\,\mathrm{e}^{\alpha + i\beta}, \ (\zeta_0 : \text{complex constant}(|\zeta_0| \ll 1)),$$

$$\Re(\zeta_0) < 0, \ \Im(\zeta_0) \geq 0, \ \alpha \geq 0,$$

where $\alpha = 0$ corresponds to the airfoil surface. The point $\alpha + i\beta = \pi i$ stands for the leading edge, and that $\alpha + i\beta = 0$ the trailing edge. The space should be univalent, the sufficient condition of which is

$$1 - c_1 - 2\,c_2 = 0, \ |c_2| \ll 1,$$

which applies hereafter. The constant q is so chosen as

$$\Re\left\{z(\alpha = 0, \beta = 0) - z(\alpha = 0, \beta = \pi)\right\} = 1.$$

The inclination of the line from the leading edge to the trailing edge is denoted to be ψ_0, i.e.

$$\tan\psi_0 \equiv \arg(z\,(\alpha = 0, \beta = 0) - z(\alpha = 0, \beta = \pi)).$$

The chord length L_0 (the distance between the leading edge and the trailing edge) is given by

$$L_0\ \cos\psi_0 = L.$$

2.2. Characteristics of configuration

In case of $|c_2|$, $|\zeta_0| \ll 1$,

$$q \approx \frac{1}{4}\,(1 + c_2)\,,$$

$$\psi_0 \approx \Im\left({\zeta_0}^2 - 2\,c_2\,\zeta_0\right).$$

Profile of the thickness H of the airfoil

$$x \approx \frac{1}{4}\left\{2\cos\beta + 2\Re(\zeta_0)\ \sin^2\beta + c_2(1 - 2\cos\beta + \cos^2\beta)\right\},$$

$$H \approx \{c_2 - \Re(\zeta_0)\} \sin\beta(1-\cos\beta),\ (0 \le \beta \le \pi),$$

$$H_{\max} \approx \frac{3\sqrt{3}}{4}\{c_2 - \Re(\zeta_0)\} \quad \text{at } \cos\beta = -1/2.$$

Camber line:

$$x \approx \frac{\cos\beta}{2},$$

$$y \approx \frac{1}{2}\,\Im(\zeta_0)\ \sin^2\beta.$$

Radius of curvature of the airfoil, R, at the leading edge:

$$R \approx \frac{2\,|\zeta_0 - c_2 + 2{\zeta_0}^2 - 4\,c_2\zeta_0|^3}{\left|\Re(\zeta_0 - c_2 + 2\,{\zeta_0}^2) + 2|\zeta_0|^2 - 10\,c_2\Re(\zeta_0) + 4\,{c_2}^2\right|}.$$

Figure 1 shows an example of a configuration of the airfoils (x_ℓ, y_ℓ : Cartesian coordinate at the leading edge).

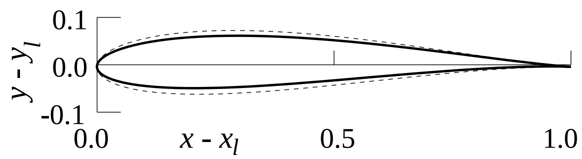

Figure 1: Example of configuration $\zeta_0 = -0.092 + 0.03\,i$
—: $c_2 = 0$, $R = 0.017$; - - - : $c_2 = 0.02$

2.3. Basic equations for the fluid flow

The equation of dimensionless vorticity transport is

$$J\frac{\partial\zeta}{\partial t} + \frac{\partial(\zeta,\psi)}{\partial(\alpha,\beta)} = \frac{1}{Re}\left(\frac{\partial^2\zeta}{\partial\alpha^2} + \frac{\partial^2\zeta}{\partial\beta^2}\right). \tag{1}$$

The relation between vorticity ζ and a stream function ψ is

$$J\zeta + \frac{\partial^2\psi}{\partial\alpha^2} + \frac{\partial^2\psi}{\partial\beta^2} = 0, \tag{2}$$

$$J \equiv \frac{\partial(x,y)}{\partial(\alpha,\beta)} = \left|\frac{dz}{d(\alpha+i\beta)}\right|^2,$$

where Re stands for a Reynolds number defined by $Re \equiv \rho U_\infty L/\mu$, (ρ: density of fluid, μ: viscosity, U_∞: uniform flow speed).

2.4. Boundary conditions

Velocity potential function $f(\alpha + i\beta)$ corresponding to the flow direction ϕ is

$$f(\alpha+i\beta) = q\,|1-\zeta_0| \; \times \left[2\cosh\omega + \left(\frac{1}{1-\epsilon_2\cosh 2\omega} - 1 \right) + B\,i\,(\alpha+i\beta) \right],$$

$$\omega \equiv \alpha + i\beta + i\beta_0 - i\phi, \beta_0 \equiv \arg(1-\zeta_0);\; \epsilon_2, B : \text{real}.$$

Potential flow assumption at $\alpha = \alpha_\infty \equiv c/\sqrt{Re}$, c: real positive suitably selected constant (currently $c = 5$) is given by

$$\frac{\partial}{\partial\alpha}\psi(\alpha=\alpha_\infty,\beta) = \Im f'(i\beta),$$

$$\zeta(\alpha=\alpha_\infty,\beta) = 0.$$

A necessary condition is $(\partial/\partial\alpha)\zeta(\alpha = \alpha_\infty, \beta) = 0$. No slip conditions on the surface ($\alpha = 0$) gives

$$\frac{\partial}{\partial\alpha}\psi(0,\beta) = 0$$

and without loss of generality it is assumed

$$\psi(0,\beta) = 0.$$

Continuity of the potential flow at the trailing edge gives

$$f'(0) = 0.$$

Also doubly connectedness of the domain through no slip flow gives

$$\oint_{\alpha=0} \frac{\partial\zeta}{\partial\alpha}\,d\beta = 0.$$

2.5. Spectral decomposition

Fourier decomposition applies:

$$\begin{bmatrix} \psi \\ \zeta \end{bmatrix} = \sum_{n=1}^{\infty} \begin{bmatrix} \psi_{sn}(\alpha,t) \\ \zeta_{sn}(\alpha,t) \end{bmatrix} \sin n\beta + \sum_{n=0}^{\infty} \begin{bmatrix} \psi_{cn}(\alpha,t) \\ \zeta_{cn}(\alpha,t) \end{bmatrix} \cos n\beta.$$

Equations (1)–(2) can be decomposed into each Fourier component.

2.6. Discretization in space

In the coordinate α, any finite difference approximation with non-uniform grid spacing may apply. Here the following to the n-th grid point applies:

$$\alpha_n = h\left(\frac{\sinh(n-1)\gamma}{\sinh\gamma} + 1\right) + \alpha_0,$$

where h, γ : real constants > 0.

2.7. Numerical integration with respect to time

A semi-implicit scheme is applied to get a steady-state solution with a suitably given initial condition.

3. Results

3.1. Force and moment

The dimensionless force, $\boldsymbol{F}$, acting on the wing (based on $\rho {U_\infty}^2 L$) is

$$\boldsymbol{F} = \frac{i}{Re}\left\{\oint \frac{dz}{d(\alpha + i\beta)}\,\zeta\, d\beta - \oint z\frac{\partial\zeta}{\partial\alpha}\, d\beta\right\},$$

The lift coefficient C_L is given by the component of $\boldsymbol{F}$, normal to the uniform flow direction, and the drag coefficient C_D is given by that parallel to the flow. Attack angle is given by $\phi - \psi_0$. The moment relative to the origin of z, C_M (based on $\rho {U_\infty}^2 L^2$), under a right hand coordinate system is given by

$$C_M = -\frac{1}{2Re}\oint |z|^2\frac{\partial\zeta}{\partial\alpha}\, d\beta + \frac{1}{2Re}\oint \zeta\frac{\partial}{\partial\alpha}|z|^2\, d\beta,$$

which is opposite sign to the traditional definition. Traditional lift, drag, moment coefficients are based on $(1/2)\rho {U_\infty}^2 S$ (S : circumference length), for which

$$0 < (S/2 - L)/L \lesssim 0.05 \;\text{ if }\; |\zeta_0|, |c_2| \ll 1.$$

Especially if ζ_0 is real,

$$S/L \approx 8(1+\xi)\sqrt{2\xi}\left[\frac{\sqrt{\beta^*}}{3}\{2\alpha^* F(\varphi,k) - (\alpha^*+\beta^*)E(\varphi,k)\}\right.$$
$$\left. + \frac{1+\beta^*+2\alpha^*}{3}\sqrt{\frac{1+\beta^*}{1+\alpha^*}}\right],$$

$$\beta^* \equiv \frac{1}{16\xi}\left\{1 - 6\xi + \sqrt{(1-6\xi)^2 - 32\xi^3}\right\},$$

$$\alpha^* \equiv \frac{\xi}{8\beta^*},\ \varphi = \tan^{-1}(1/\sqrt{\alpha^*}),\ k = \sqrt{(\beta^* - \alpha^*)/\beta^*},$$

$$\xi \equiv |\zeta_0| + c_2\ (> 0),$$

where $F(\cdot,\cdot), E(\cdot,\cdot)$: elliptic integral of the first, and of the second kind respectively.

3.2. Force characteristics

Figure 2 shows force characteristics against the attack angle.

Figure 3 shows moment characteristics against the attack angle. Present numerical examples shown are for $\epsilon_2 = -0.1$ unless otherwise stated, e.g. [12].

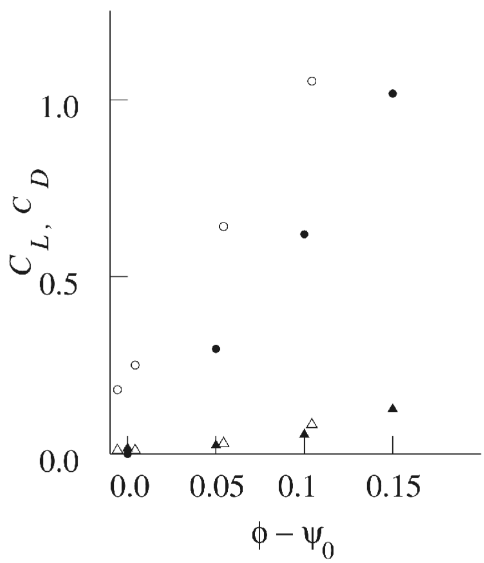

Figure 2: $\phi - \psi_0$: angle of attack • : C_L, ▲ : C_D : $\zeta_0 = -0.092$ ($c_2 = 0$) ○ : C_L, △ : C_D : $\zeta_0 = -0.092 + 0.03i$, $H_{\max} = 0.11$, $Re = 10^6$, $\epsilon_2 = -0.1$

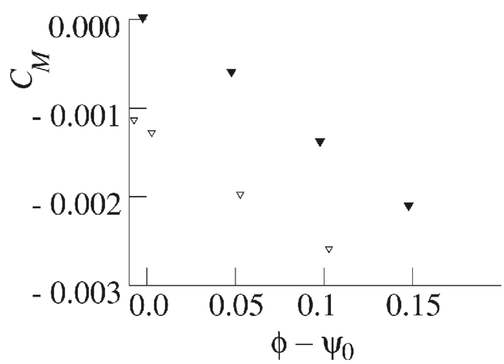

Figure 3: $\phi - \psi_0$: angle of attack ▼ : C_M : $\zeta_0 = -0.092$ ($c_2 = 0$, $Re = 10^6$) ▽ : C_M : $\zeta_0 = -0.092 + 0.03i$ ($c_2 = 0$, $Re = 10^6$)

Figure 4 shows the lift dependency on c_2.

Figure 5 shows comparison of C_L vs. angle of attack with experimental ones.

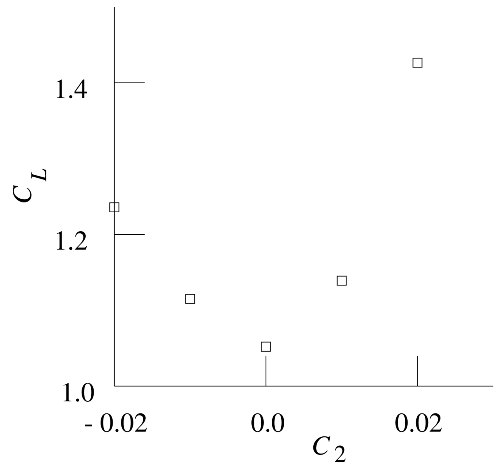

Figure 4: $\phi = 0.1$ $\zeta_0 = -0.092 + 0.03i$ $Re = 10^6$, $\epsilon_2 = -0.1$

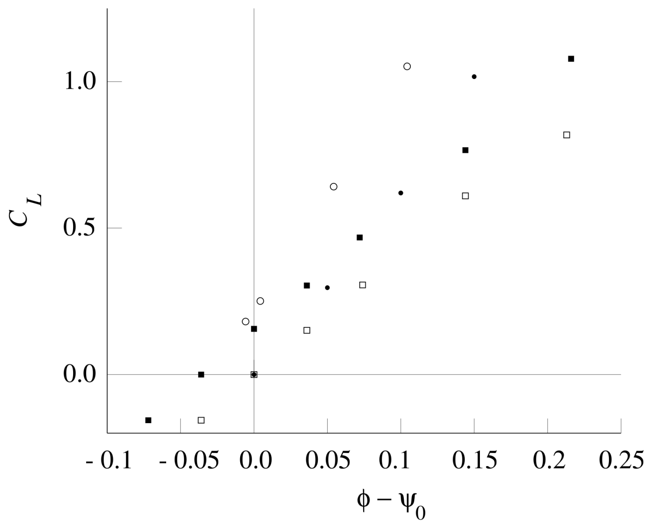

Figure 5: Comparison $\circ$: $\zeta_0 = -0.092 + 0.03i$, $H_{\max} = 0.11$ $c_2 = 0$, $Re = 10^6$ $\bullet$: $\zeta_0 = -0.092$, $c_2 = 0$, $Re = 10^6$ $\square$: NACA 0009 [4] $\blacksquare$: NACA 2309 [4]

3.3. Correlation between lift and drag coefficients

Figure 6 shows correlation between lift and drag coefficients.

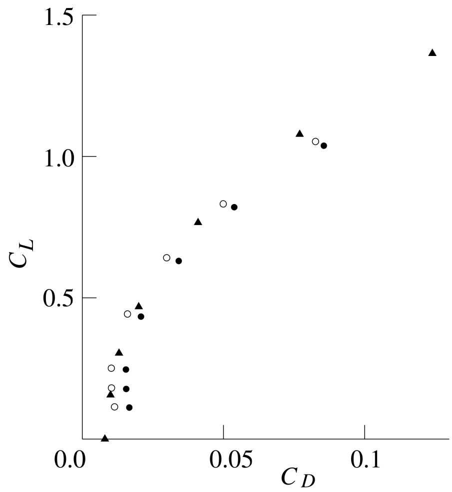

Figure 6: Comparison ▲: NACA 2309, $Re = 1.8 \times 10^5$ [4], $\circ$: $\zeta_0 = -0.092 + 0.03i, c_2 = 0,\ H_{\max} = 0.11,\ Re = 10^6$, $\bullet$: $\zeta_0 = -0.092 + 0.03i,\ c_2 = 0, Re = 10^5$

4. Conclusions

Spectral finite difference schemes give good solutions for aerodynamic characteristics of Joukowsky like wings, with configuration characteristics.

References

[1] M. M. Munk. The Air Forces on a Systematic Series of Biplane and Triplane Cellule Model. N.A.C.A. Report No. 256, 1927.

[2] E. N. Jacobs. Tests of Six Symmetrical Airfoils in the Variable Density Wind Tunnel. N.A.C.A. Technical Notes No. 385, 1931.

[3] E. M. Jacobs, I. H. Abbott. The N.A.C.A. Variable-Density Wind Tunnel. N.A.C.A. Technical Report No. 416, 1933.

[4] E. A. Jacobs, K. E. Ward, R. M. Pinkerton. The Characteristics of 78 related airfoil section from tests in the Variable-Density Wind Tunnel. N.A.C.A. Report No. 460, 1933.

[5] E. A. Jacobs, A. Sherman. Airfoil Section Characteristics as Effected by Variations of the Reynolds Number. N.A.C.A. Report No. 586, 1937.

[6] R. H. Neely, T. V. Bollech, G. C. Westrick, R. R. Graham. Experimental and Calculated Characteristics of Several NACA 44-Series Wings with Aspect Ratios of 8, 10 and 12 and Taper Ratios of 2.5 and 3.5. N.A.C.A. Technical Note No. 1270, 1947.

[7] H. C. Garner, A. S. Baston. Measurement of Lift, Pitching Moment and Hinge Moment on a Two-dimensional Cumbered Airfoil to assist the Estimation of Camber Derivatives. A.R.C. Technical Report No. 2946, 1952.

[8] M. M. Munk. General Theory of Thin Wing Sections. N.A.C.A. Report No. 142, 1923.

[9] T. Theodorsen. Theory of Wing Sections of Arbitrary Shape. N.A.C.A. Report No. 411, 1933.

[10] I. H. Abbott, A. E. Doenhoff. Theory of Wing Sections, Including a Summary of Airfoil Data. Dover Pub., 1949.

[11] M. S. Selig, J. J. Guglielmo, A. P. Broeron, P. Giguere. Summary of Low-Speed Airfoil Data, Vol. 1, Virginia, USA, Soar Tech Publications, 1995.

[12] D. Akita, Y. Mochimaru. Numerical simulation of a flow past an elliptic cylinder at high Reynolds numbers. *CMMPG*, **1** (2015), 1–7.

Yoshihiro Mochimaru
Tokyo Institute of Technology
57-121, Yamaguchi, Tokorozawa
Saitama 359-1145, Japan
e-mail: `ymochima-1947@cx.117.cx`